Effects of a Carane Derivative Local Anesthetic on a Phospholipid Bilayer Studied by Molecular Dynamics Simulation

M. Pasenkiewicz-Gierula,* T. Róg,* J. Grochowski,† P. Serda,† R. Czarnecki,‡ T. Librowski,‡ and S. Lochyński§
*Department of Biophysics, Institute of Molecular Biology and Biotechnology, Jagiellonian University, Kraków, Poland; †Regional Laboratory of Physicochemical Analysis, Jagiellonian University, Kraków, Poland; ‡Department of Pharmacodynamics, Medical College of the Jagiellonian University, Kraków, Poland; and §Institute of Organic Chemistry, Biochemistry and Biotechnology, Wrocław University of Technology, Wrocław, Poland

ABSTRACT Molecular dynamics (MD) simulations of two hydrated palmitoyloleoylphosphatidylcholine (POPC) bilayers each containing eight carane derivative (KP-23) local anesthetic (LA) molecules in neutral (POPC-LA) or protonated (POPC-LAH) forms were carried out to investigate the effect of KP-23 and its protonation on the bilayer. 3-ns trajectories were used for analyses. A pure POPC bilayer was employed as a reference system. In both POPC-LA and POPC-LAH systems a few KP-23 molecules intercalated into the bilayer and moved near the bilayer/water interface. They were located on the hydrophobic core side of the interface in the POPC-LA bilayer, but on the water phase side in the POPC-LAH bilayer. The order of the POPC chains was higher in the POPC-LA bilayer than in the pure POPC bilayer and was lower in the POPC-LAH bilayer. Interactions between polar groups of KP-23 and POPC or water were responsible for a lower hydration of POPC headgroups in POPC bilayers containing KP-23 than in the pure POPC bilayer. KP-23 molecules were found to form aggregates both in POPC-LA and POPC-LAH bilayers. Due to higher amphiphilicity of LAH, the LAH aggregate was more micelle-like and larger than the LA one. The results demonstrate the rapid timescales of the initial processes that take place at and near the bilayer interface as well as details of the atomic level interactions between local anesthetic and the lipid matrix of a cell membrane.

INTRODUCTION

Most local anesthetics (LA) in use at the present time are amphiphilic molecules with an ionizable amino group and a lipophilic aromatic ring. They block the initiation or conduction of nerve impulses brought about by transport of extracellular sodium to the cytosol through the sodium channel, which is an integral plasma membrane protein. Molecular mechanisms of local anesthesia have yet to be clarified although several theories have been proposed to account for them (Gupta, 1991; Frangopol and Mihăilescu, 2001). At present, a commonly accepted scheme is that local anesthetics diffuse in the uncharged form across the nerve sheath and nerve membrane; re-equilibrate between the uncharged and cationic forms on the axoplasmatic surface of the nerve membrane; and penetrate into and attach to a receptor at the site within a sodium channel. Whether the site comprises pure lipids or protein amino acid residues or perhaps both, is still unknown. A specific binding site within the protein for all or most local anesthetics seems unlikely because of substantial differences in their chemical structure. This variety, together with a correlation between the potency of LA and its lipophilicity, strongly suggests that LA-lipid interaction may play a significant role in local anesthesia. The amphiphilic character of LA molecules indicates that they may be located in the interfacial region of the membrane in the initial stage of their action. Such a location would allow them to affect the hydration of the membrane surface as well as the order and dynamics of the hydrophobic core of the membrane.

The effects of LA on a phospholipid bilayer and LA-lipid interactions have been studied intensively by various workers. The earlier studies of de Paula and Schreier (1996) and of Ohki and Ohshima (1996) indicated that both charged and neutral LAs bind to the bilayer, the former in the headgroup region, the latter more deeply in the hydrophobic core but near the bilayer/water interface. Recent results of research that focused on the effects of local anesthetics on the membrane/water interface have been summarized by Frangopol and Mihăilescu (2001). They demonstrated a partial intercalation of LA into the lipid bilayer; an LA-induced increase of the mean distance between lipid molecules; decreased intercalation upon LA protonation; certain nonspecific interactions between LA and bilayer lipids; and the LA decreased fluidity of the erythrocyte membrane. Used clinically, uncharged local anesthetics were observed to decrease molecular organization in the bilayer (de Paula and Schreier, 1995; Pinot et al., 2000) and to increase the organization of micelles (Teixeira et al., 2001). The site of the largest perturbing effect depended on the drug hydrophobicity but was always found close to the upper positions in the phospholipid hydrocarbon chain. Ueda et al. (1994) demonstrated that LAs released PC-bound water. By forming hydrogen (H-) bonds with PC phosphate and carbonyl oxygen atoms, LA replaces water molecules that were H-bonded to these groups. Their experiments also showed cooperative binding of LA to the membrane/water interface and suggested a correlation between anesthetic potency and its interfacial condensation. Matsuki et al.

Submitted October 18, 2002, and accepted for publication April 11, 2003.
Address reprint requests to Marta Pasenkiewicz-Gierula, Jagiellonian University, Institute of Molecular Biology and Biotechnology, ul. Gronostajowa 7, Kraków, Poland 30-387. Tel.: 48-12-252-6518; Fax: 48-12-252-6902; E-mail: mpg@mol.uj.edu.pl.

0006-3495/03/08/1248/11 $2.00

(1998) demonstrated that LAs self-condense into micelle-like aggregates.

Based on his comprehensive studies of anesthesia, Ueda (2001) concluded that anesthetics are nonspecific drugs that affect both proteins and lipid assemblies by increasing their volume.

$C_{16}H_{30}O_2N_2 \cdot HCl$ (KP-23) is synthesized from amino-hydroxyiminocarane, the main component of the *Pinus sylvestris* essential oil (Siemieniuk et al., 1992). It is a potent local anesthetic of surprisingly long-lasting activity (Czarnecki et al., 1992), but the mechanism of its action at the molecular level is not known. The KP-23 molecule consists of a lipophilic carane head (a saturated hydrocarbon ring) and an isopropyl side chain (Fig. 1 *b*). X-ray crystallographic studies revealed that the KP-23 molecule crystallizes in epimeric form in the triclinic P1 space group and possesses four chiral centers (Czarnecki et al., 1992). Two epimers of KP-23, specifically KP-23R and KP-23S, present in the asymmetric unit cell have identical 1R, 3R, and 6S absolute configuration at the chiral centers in the carane moiety but opposite absolute configuration at the chiral center in the side chain. They also have nearly identical conformations except for the N1-O1-C11-C12 torsion angle (compare to Fig. 1 *b*), which is ~130° and ~73° for 'R' and 'S' epimers, respectively.

Stereospecific synthesis was designed to provide homochiral forms of KP-23: KP-23R and KP-23S (Lochyński et al., 2002). Unfortunately, only the S-form has been successfully confirmed by crystal structure and phase analysis using classic and synchrotron radiation sources (Grochowski et al., 2002). To assure better solubility, both epimeric and homochiral forms of KP-23 were synthesized as a hydrochloride. In the unit cell, the two KP-23 molecules are joined by medium strength H-bonds via Cl^- and form a dimer.

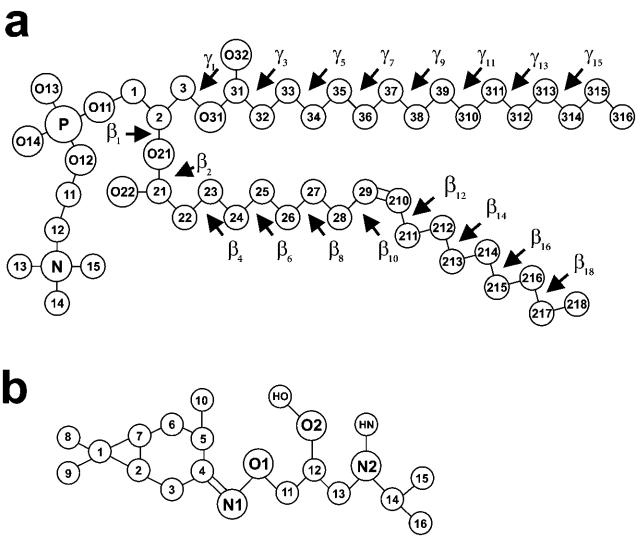

FIGURE 1 Molecular structure with numbering of atoms and torsion angles of POPC (*a*), and KP-23 (*b*) (chemical symbol for carbon atoms, C, is omitted). The chiral center in the KP-23 side chain is on C12.

In the present study, a molecular dynamics (MD) simulation was applied to investigate the effect of KP-23 on the membrane/water interface as well as the hydrocarbon chain core of a fully hydrated palmitoyloleoylphosphatidylcholine (POPC) bilayer. The effects of neutral and cationic species as well as KP-23R and KP-23S epimers were compared. This investigation is of interest because both charged and uncharged forms of local anesthetic exist at the physiological pH and because a nonstereospecific synthesis of KP-23 yields two epimers in approximately equal amounts.

METHODS

Simulation systems

Computer models of the KP-23 molecules in two epimeric forms and two protonated states were constructed on the basis of molecular structures of KP-23R and KP-23S obtained from x-ray diffraction (Czarnecki et al., 1992; Grochowski et al., 2001). The molecules as dimers and monomers in neutral and cationic forms were placed in an phosphatidylcholine (PC) bilayer membrane made of 72 POPC and 1922 water molecules (Murzyn et al., 2001) and equilibrated for 11 ns. A hydrated POPC bilayer constitutes a convenient model of a plasma membrane. Two membrane-LA systems were built, one containing eight neutral KP-23 molecules (three dimers: RS, SS, and RR, and two monomers), six H^+ and six Cl^- (POPC-LA), and the other containing eight protonated KP-23 molecules (three dimers and two monomers), and eight Cl^- (POPC-LAH). Initially, the KP-23 molecules were placed horizontally on the bilayer surface. POPC-LA and POPC-LAH systems were simulated for 10 or 5 ns, respectively. The pure POPC bilayer was used as a reference system. Details concerning the construction and the initial simulation of this bilayer are described in Murzyn et al. (2001). MD simulation of this bilayer was carried out for a total time of 15 ns. The last 4-ns fragment of its trajectory was generated using the Particle Mesh Ewald (PME) method (Essmann et al., 1995). Due to the comparative character of this study, numbers of lipid and water molecules in the three bilayers were the same. Eight KP-23 molecules and 1922 water molecules hydrating POPC-LA and POPC-LAH systems constitute 0.9% water solution; this concentration falls into the range of concentrations that have been applied in pharmacological experiments (Librowski et al., 2000). Fig. 1, *a* and *b*, show the structure and numbering of the atoms in POPC and KP-23 molecules, respectively.

Simulation parameters

For POPC, KP-23, and ions, OPLS parameters (Jorgensen and Tirado-Rives, 1988), and for water, TIP3P parameters (Jorgensen et al., 1983) were used. POPC, KP-23, H^+, and Cl^- were treated as the solute molecules and water was the solvent. The united-atom approximation was applied to the CH, CH_2, and CH_3 groups of POPC and KP-23. All polar groups of the solute and solvent molecules were treated in full atomic detail. The atomic charges of KP-23 in neutral and protonated states were obtained by minimizing the electrostatic energy with respect to these charges. The method is provided together with the Extensible Systematic Forcefield in the MSI package (DISCOVER User Guide, 1995). The numerical values for the charges are given in Table 1. Procedures for supplementing the original OPLS base with the missing parameters for the POPC headgroup have been described elsewhere by Pasenkiewicz-Gierula et al. (1999) and those for the β-chain sp2 carbon atoms by Murzyn et al. (2001). In the original OPLS set, the stretching, bending, and torsion parameters for groups containing N1 and O1 atoms in the KP-23 isopropyl side chain (compare to Fig. 1) were also missing. These parameters were set by analogy with the OPLS parameters appropriate to adenine and guanine.

TABLE 1 Atomic point charges on LA and LAH molecules in the united atom approximation

Atom	LA	LAH
C1	−0.070	−0.070
C2	−0.005	−0.005
C3	0.125	0.125
C4	0.005	0.005
C5	0.045	0.045
C6	0.046	0.046
C7	−0.017	−0.017
C8	0.038	0.038
C9	0.038	0.038
C10	0.049	0.049
N1	−0.228	−0.228
O1	−0.256	−0.255
C11	0.236	0.254
C12	0.148	0.211
O2	−0.581	−0.566
HO	0.367	0.367
C13	0.114	0.261
N2	−0.331	−0.209
HN (1, 2)	0.202	0.298, 0.298
C14	−0.0013	0.037
C15	0.044	0.139
C16	0.044	0.139

The charges were obtained for LA and LAH in the all atom model by minimizing the electrostatic energy with respect to the charges (DISCOVER User Guide, 1995). Numbering of atoms as in Fig. 1.

Simulation conditions

POPC-LA and POPC-LAH systems as well as the last 4 ns of the pure POPC bilayer were simulated using the MD Amber 5.0 packages (Case et al., 1997). Three-dimensional periodic boundary conditions with the usual minimum image convention were used. The SHAKE algorithm (Ryckaert et al., 1977) was used to preserve the bond lengths of OH, NH, and NH_2 groups of water and KP-23 molecules, and the time step was set at 2 fs (Egberts et al., 1994). As POPC-LAH and POPC-LA systems contain charged molecules and/or ions, in the simulations of the bilayers, long-range electrostatic and van der Waals interactions were evaluated by means of the PME summation method (Essmann et al., 1995). A real cutoff of 12 Å, with a β-spline interpolation order of 5, and a direct sum tolerance of 10^{-6} were used. The list of nonbonded pairs was updated every 25 steps.

The MD simulations were carried out at a constant pressure (1 atm) and at a temperature of 310 K (37°C), which is above the main phase transition temperature for a POPC bilayer (−5°C) (Seelig and Waespe-Šarčević, 1978). The temperatures of the solute and solvent were controlled independently by the Berendsen method (Berendsen et al., 1984). The applied pressure was controlled anisotropically, each direction being treated independently with the trace of the pressure tensor kept constant for 1 atm, again using the Berendsen method (Berendsen et al., 1984). The relaxation times for temperatures and pressure were set at 0.4 and 0.6 ps, respectively.

RESULTS

Equilibration of the membrane systems

The approach to the equilibrium state of the POPC bilayer containing neutral KP-23 molecules (POPC-LA system) in the liquid-crystalline phase was observed from the onset of simulation until 10 ns. The following parameters of the system were monitored: the temperature (Fig. 2 *a*), potential energy (Fig. 2 *b*), and surface area per PC headgroup (Fig. 2 *c*). Similar time profiles were obtained for the POPC bilayer containing protonated KP-23 molecules (POPC-LAH system) and simulated for 5 ns (data not shown). From the time profiles it was concluded that in the POPC-LA and POPC-LAH systems the parameters reached stable average values after ~5.0 and ~2.0 ns, respectively. Thus, for analyses below, last 3-ns fragments of POPC-LA, POPC-LAH, and pure POPC trajectories were used. Errors in the derived average values are standard error estimates obtained from the block averaging procedure.

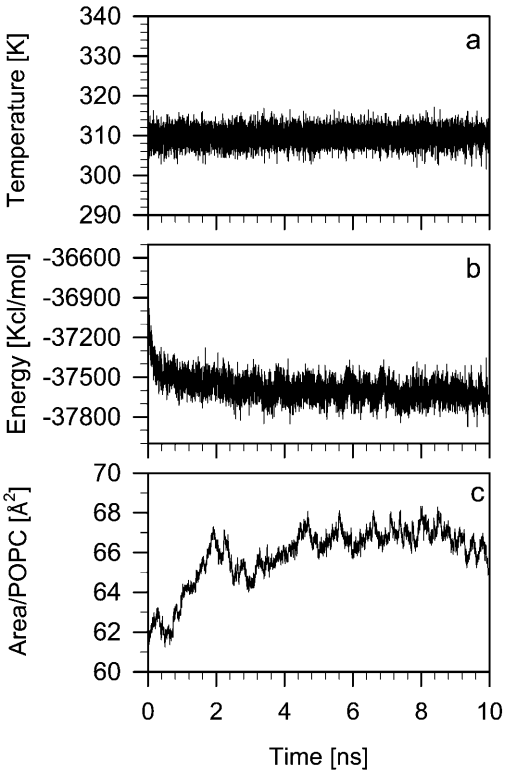

FIGURE 2 Diagrams showing the time development of the temperature (*a*), potential energy (*b*), and surface area per POPC headgroup (*c*) in the POPC-LA bilayer. The equilibrium average surface area is 66 ± 1 Å^2.

KP-23 in the POPC bilayer

Location of LA and LAH molecules in the POPC bilayer

Our test simulations of POPC bilayers containing lidocaine and neutral KP-23 molecules, which used a 12 Å cutoff for evaluation of long-range interactions, suggested that the molecules preferentially localize in or near the bilayer/water interface within the first nanoseconds of the MD simulation. In the present study, which employed the PME method for evaluation of long-range interactions (see Methods section) it is important to know if LA and LAH molecules spontaneously enter the PC bilayer and diffuse through it. For this reason, in the initial step of our construction of the

POPC-LA and POPC-LAH bilayers, KP-23 molecules (both in dimeric and monomeric forms) were placed horizontally on the POPC bilayer surface, four on top of each leaflet. Next, water molecules were added to the bilayers. Snapshots of POPC-LA and POPC-LAH bilayers in the initial states, each containing 8 KP-23 molecules, are shown in Fig. 3, *a* and *c*. After a few hundred picoseconds of the MD simulation, the chlorine ions that participated in dimer formation of both neutral and protonated KP-23 molecules diffused away and the dimers dissociated.

Fig. 4 *a* shows changes in time of the location of the center of mass of the LA molecules along the membrane normal (*z*-axis). In this figure, the horizontal lines labeled ''O32'' and ''N'' indicate time and ensemble average positions of the carbonyl oxygen O32 and the choline nitrogen atoms (compare to Fig. 1), respectively, and approximate the width of the bilayer/water interface. During the course of the MD simulation of 10 ns, practically none of the LA molecules remained at its initial position. Four molecules that detached from the bilayer surface, within ~3 ns, formed a stable aggregate immersed in water. The fifth molecule that detached, diffused across the water phase and entered the other leaflet. This, and the remaining three molecules, penetrated the bilayer/water interface and located, at least partially, in the nonpolar region of the bilayer (Fig. 3 *b*). Crossing times of the interface and water phase were of the order of 200–400 ps. The snapshot of the POPC-LA bilayer after 10 ns of the MD simulation is shown in Fig. 3 *b*.

Fig. 4 *b* shows changes in time of the location of the center of mass of the LAH molecules along the *z*-axis. Within ~500 ps of the MD simulation, two of four LAH molecules detached from the surface of one leaflet; the third one detached after 3 ns. These molecules diffused across the bilayer water phase and aggregated with the four molecules initially placed on top of the second leaflet. Of the latter four LAH molecules, only one remained in its initial location. This molecule anchored the seven-molecule aggregate to the bilayer surface via three H-bonds formed between NH_2 and OH groups and phosphate oxygen atoms of three PC molecules (Fig. 5 *c*). Of the eight LAH molecules in the POPC-LAH bilayer, only one remained in the monomeric state. In contrast to the neutral KP-23 molecules, none of the

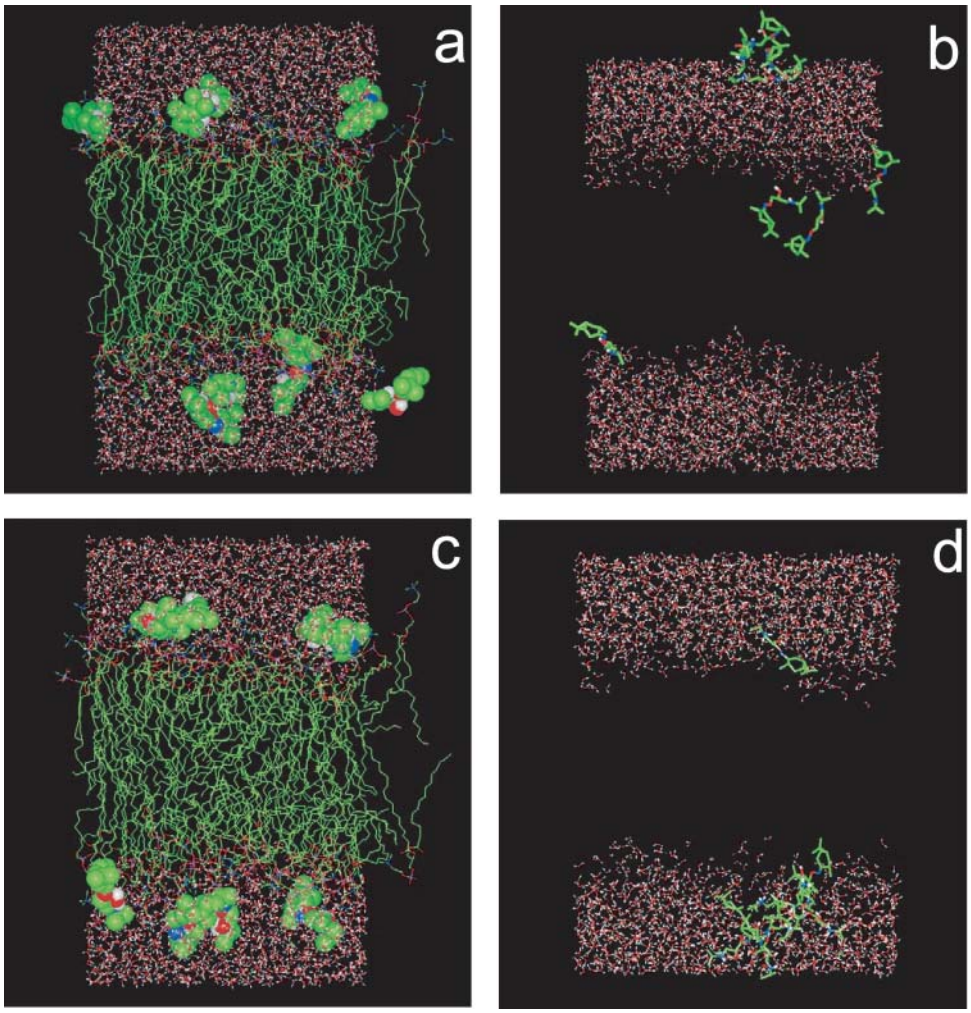

FIGURE 3 Snapshots of the POPC-LA bilayer at 0 ps (*a*) and 10 ns (*b*) of the MD simulation, and of the POPC-LAH bilayer at 0 ps (*c*) and 5 ns (*d*) of the MD simulation. In (*a*) and (*c*) KP-23 molecules are shown in the CPK representation. In (*b*) and (*d*) KP-23 molecules are shown in the stick representation; to better show the location of KP-23 in the bilayer in (*b*) and (*d*) POPC molecules were removed. All molecules are in standard colors (*C* is *green*, *O* is *red*, *N* is *blue*, *H* is *white*, and *P* is *pink*).

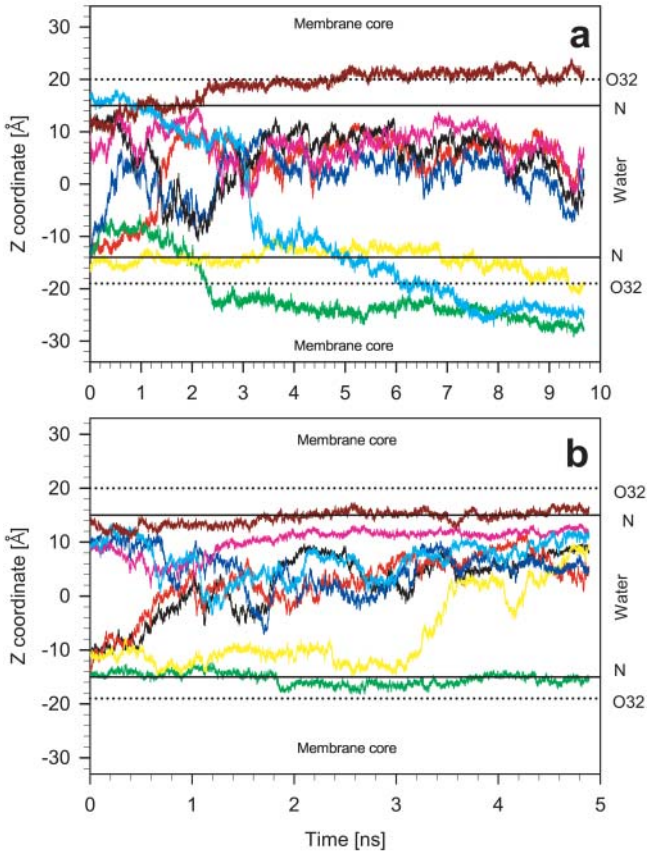

FIGURE 4 Time profiles of the vertical positions (z-axis) of the center of mass of eight neutral (*a*) and protonated (*b*) KP-23 molecules in POPC-LA and POPC-LAH bilayers. The center of the vertical axis (zero) is the middle of the bilayer water phase. Horizontal lines labeled ''O32'' and ''N'' indicate time and ensemble average positions of the carbonyl oxygen O32 and the choline nitrogen atoms (compare to Fig. 1), respectively, and indicate the width of the bilayer/water interface. ''Membrane core'' labels the hydrocarbon core region and ''Water'' the water phase of the bilayer.

eight protonated KP-23 molecules moved to the nonpolar region of the POPC-LAH bilayer within 5 ns. The snapshot of the POPC-LAH bilayer after 5 ns of the MD simulation is shown in Fig. 3 *d*. Localization of LA and LAH molecules in POPC bilayers at the end of respective MD simulations seems to be uncorrelated with their chirality and starting conformations.

Interactions between LA and POPC

Within 10 ns of the MD simulation, four of the eight neutral KP-23 molecules partially entered the nonpolar region of the bilayer (Fig. 3 *b*). Polar groups (OH and NH) of three of them formed links with polar groups (phosphate and carbonyl) of POPC via H-bonds (e.g., Fig. 5 *a*) or charge interactions. These molecules stayed close to the bilayer/water interface (Fig. 3 *b*). One LA molecule that did not make links with POPC polar groups entered deeper into the hydrophobic core of the bilayer.

LA and POPC also established tight van der Waals contacts. Examples of such contacts leading to a POPC chain bending around a carane head and POPC chain alignment along an LA side chain can be seen in Fig. 5 *b*. A similar alignment is known to take place between dimyristoylphosphatidylcholine alkyl chains and cholesterol in a dimyristoylphosphatidylcholine-cholesterol bilayer membrane (Róg and Pasenkiewicz-Gierula, 2001a).

Interactions between LAH and POPC

During the 5-ns simulation of the POPC-LAH system, none of the protonated KP-23 penetrated the bilayer deep enough to directly interact with POPC hydrocarbon chains (Fig. 3 *d* and 4 *b*). A protonated KP-23 has the potential to make more H-bonds and charge interactions with POPC than a neutral one. However, because seven LAH molecules formed an aggregate, interactions between polar groups of these LAH molecules and POPCs were not numerous. Only one LA molecule fully satisfied its H-bonding potential forming three simultaneous H-bonds (two via NH_2 and one via OH groups) with phosphate groups of three POPC molecules (Fig. 5 *c*).

Interactions between KP-23 molecules

Both 4-molecule LA and 7-molecule LAH aggregates were stabilized predominantly by hydrophobic interactions. Their interiors did not contain water molecules and polar groups compensated each other mainly by intramolecular electrostatic interactions. In the LA aggregate, the molecules were in a head-to-tail-like arrangement (Fig. 5 *e*). LAH molecules, which are more amphiphilic than their neutral counterparts, formed a micelle-like aggregate (Fig. 5 *f*). The lipophilic rings comprised the inner core of the aggregate and fragments of the positively charged side chains were exposed to water.

As can be seen from Fig. 4, 4-molecule LA and 7-molecule LAH aggregates formed within 3–4 ns and remained stable for the remaining MD simulation time. KP-23 molecules in a monomeric state resided in the water phase for a very short time. So, before final aggregates developed, the molecules formed smaller aggregates.

Interactions between KP-23 and water

In the POPC-LA system, the four molecules that intercalated into the bilayer practically did not make H-bonds with water (only one made such bonds), whereas in the POPC-LAH system, OH and NH_2 groups of LAH side chains did make such bonds (Fig. 5 *d*). Also, aggregated LA molecules made H-bonds with water in much smaller numbers than aggregated LAH molecules. The average number of H-bonds between LA and water was 1.3, and between LAH and water was 2.1. Nonpolar groups of LA and LAH that were exposed

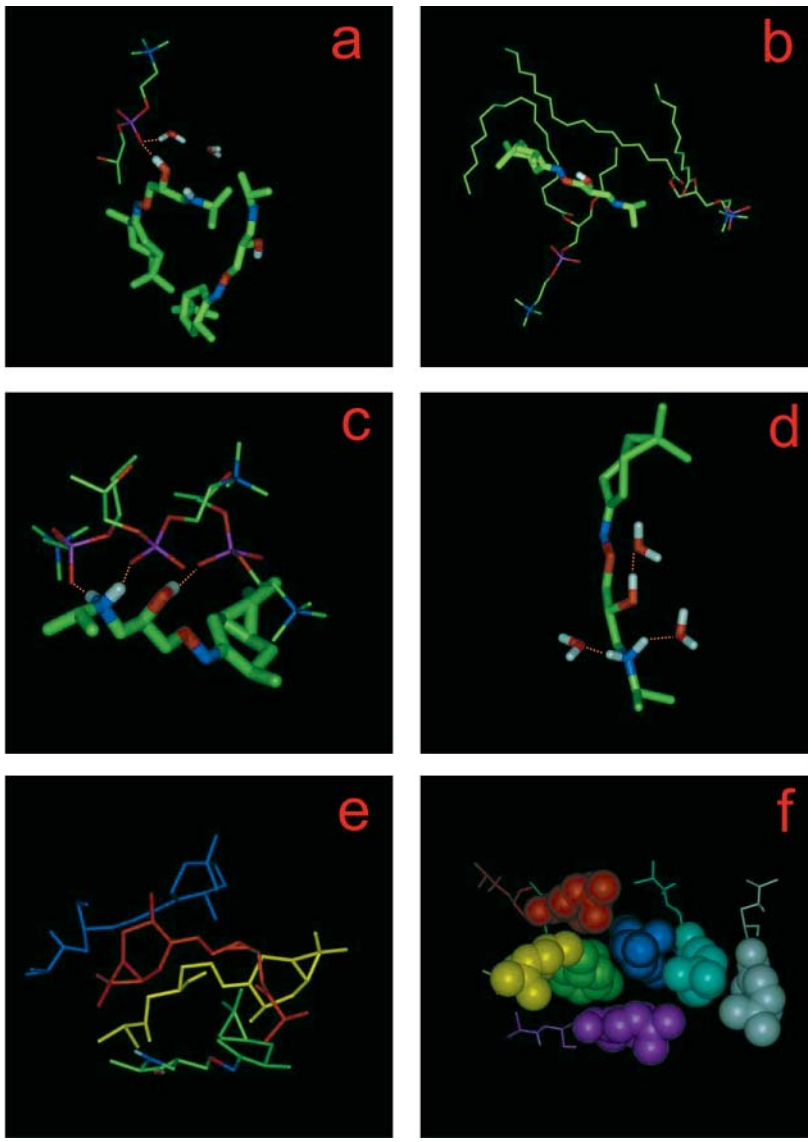

FIGURE 5 Examples of PC–KP-23, water–KP-23, and KP-23–KP-23 interactions in the membrane. (*a*) H-bond between an OH group of LA and a PC phosphate oxygen (Op) atom; a water molecule that is H-bonded to the same Op is also shown. (*b*) Alignment and bending of PC alkyl chains along the side chain and around the rings of LA, respectively; (*c*) three H-bonds between OH and NH_2 groups of one LAH molecule and Op atoms of three POPC molecules; (*d*) H-bonds between LAH and water. KP-23 and water molecules are shown in the stick representation; and POPC molecules and their fragments are shown in the line representation. (*e*) Four-molecule LA and (*f*) seven-molecule LAH aggregates. To better show the arrangement of molecules, each LA and LAH molecule is shown in a different color; LAH carane rings are in the CPK representation.

to water perturbed the H-bond network of surrounding water molecules forcing them to form clathrates. Due to a small number of KP-23–lipid interactions and KP-23–water H-bonds, precise evaluation of their lifetime is not possible. Nevertheless, one expects the lifetimes to be of the same order as the average lifetimes of PC-PC and PC-water interactions; namely, 150–250 ps and 50–100 ps, respectively (Pasenkiewicz-Gierula et al., 1999).

Effects of KP-23 on a POPC bilayer

Bilayer/water interface

The interfacial region of a PC bilayer is characterized by the number of interactions between water molecules and PC polar groups as well as those between neighboring PC headgroups (Pasenkiewicz-Gierula et al., 1997, 1999). These numbers are related to the cross-sectional surface area occupied by a PC molecule in the bilayer (Murzyn et al., 2001). Intercalation of other molecules into a PC bilayer generally increases the average distance between PC headgroups but may affect the PC hydrocarbon chains differently. Murzyn et al. (2001) showed that hydration of the bilayer surface increases with increasing surface area per PC brought about by an increased accessibility of PC polar groups to water. On the other hand, the number of direct and water-mediated PC-PC interactions decreases due to an increased PC-PC spacing. The average surface area available to a PC headgroup is 64 ± 1 Å^2 in POPC and 66 ± 1 Å^2 in POPC-LA and POPC-LAH bilayers (Table 2). It follows that an average lateral PC-PC spacing is larger in POPC bilayers containing KP-23 molecules than in the pure POPC bilayer.

Figs. 3 and 4 indicate a nonsymmetric distribution of KP-23 molecules between bilayer leaflets both in POPC-LA and

TABLE 2 Average values of parameters

	Area/PC ± 1	S_{mol} ± 0.01		Tilt (°) ± 0.5		No. *Gauche* ± 0.05	
	[Å^2]	$\beta(f, m)$	$\gamma(f, m)$	β	γ	β	γ
POPC	64	0.27	0.32	21.0	24.0	3.49	3.12
POPC-LA	66	0.30 (0.27, 0.32)	0.33 (0.33, 0.35)	21.0	24.0	3.50	3.12
POPC-LAH	66	0.25 (0.20, 0.27)	0.27 (0.23, 0.29)	23.0	26.5	3.50	3.24

The surface area per PC (*Area/PC*); molecular order parameter (S_{mol}) of β- and γ-chain; tilt angle (*Tilt*) of β- and γ-chain; number of *gauche* conformations per β- and γ-chain in pure POPC, POPC-LA, and POPC-LAH bilayers, and in leaflets containing more (m) and fewer (f) KP-23 molecules of POPC-LA and POPC-LAH bilayers (f, m). Errors in the average values are standard error estimates.

POPC-LAH systems. After equilibration, in each bilayer there is one leaflet that contains only one KP-23 molecule. So, to understand the effect of KP-23 on the bilayer each bilayer leaflet was analyzed separately and compared with a pure POPC bilayer. Due to the method of calculating the pressure, the surface area in both leaflets was the same. In a pure POPC bilayer, the difference in values of entities in Tables 2 and 3 derived for ''upper'' and ''lower'' leaflets were within estimated errors; therefore only single average numbers are given.

Hydration of PC molecules in each leaflet of POPC-LA and POPC-LAH bilayers is compared with that for the pure POPC bilayer in Table 3. In leaflets containing fewer KP-23 molecules there are more H-bonded water molecules per PC than in leaflets containing more; however, differences between the numbers in the three bilayers are small. Much larger differences are found for numbers of water molecules that clathrate the choline moiety (Table 3). Again, leaflets containing fewer KP-23 molecules are more similar to the pure POPC bilayer. In the POPC-LAH bilayer the difference in PC hydration between leaflets is larger than in the POPC-LA bilayer. A decreased number of water molecules hydrating a PC headgroup in POPC-LA and POPC-LAH bilayers is accompanied by an increased number of PC-PC links via Coulomb interactions (charge pairs) (Table 3). The increase is higher in leaflets containing more KP-23 molecules. These indicate that both neutral and protonated KP-23 molecules partially dehydrate the bilayer surface or shield it from water. Indeed, an increased number of charge pairs between PC molecules was observed in the process of bilayer fusion brought about by the gradual dehydration of the bilayer surface (Ohta-Ino et al., 2001).

Hydrophobic core of a PC-LA bilayer

The hydrophobic core of a bilayer in the liquid-crystalline state is characterized by a disorder of hydrocarbon chains. Quantities that describe the disorder are the number of *gauche* conformers/chain, the profile of *gauche* probability along a PC chain, the molecular order parameter profile, and the chain tilt angle. Each bilayer leaflet in POPC-LA and POPC-LAH systems was analyzed separately for the reason given above.

Molecular order parameter of PC alkyl chains

The molecular order parameter for the n^{th} segment of an alkyl chain, S_{mol}, is defined through (Hubbell and McConnell, 1971)

$$S_{mol} = \frac{1}{2}\langle 3\cos^2\theta_n - 1\rangle,$$

where θ_n is the instantaneous angle between the n^{th} segmental vector, i.e., the (C_{n-1}, C_{n+1}) vector linking $n-1$ and $n+1$ carbon (C) atoms in the alkyl chain and the bilayer normal; and $\langle\ \rangle$ denotes both the ensemble and the time average. S_{mol} profiles along the β- and γ-chain in POPC-LA, POPC-LAH, and POPC bilayers averaged over both leaflets are shown in Fig. 6, *a* and *b*, respectively. The order parameter is used to characterize both experimentally (e.g., Seelig and Seelig, 1980) and computationally (e.g., Heller et al., 1993) the order of alkyl chains in membranes. Fig. 6, *c* and *d*, show S_{mol} profiles along the β- and γ-chain, respectively, in leaflets containing more KP-23 molecules of POPC-LA and POPC-LAH systems. Average values of S_{mol} are given in Table 2. S_{mol} values in the

TABLE 3 Hydration of POPC headgroup

No./PC	POPC	POPC-LA (f, m)	POPC-LAH (f, m)
H-bonded water	4.9 ± 0.1	4.8 ± 0.1 (4.9, 4.7)	4.8 ± 0.1 (4.9, 4.6)
Choline water	6.4 ± 0.1	6.0 ± 0.1 (6.1, 5.9)	6.0 ± 0.1 (6.4, 5.6)
Bound water	11.3 ± 0.1	10.9 ± 0.1 (11.0, 10.6)	10.8 ± 0.1 (11.3, 10.2)
Water bridges	0.60 ± 0.01	0.57 ± 0.01	0.61 ± 0.01
Charge pairs	1.7 ± 0.1	2.2 ± 0.1 (2.0, 2.4)	2.2 ± 0.1 (1.8, 2.6)

Given are numbers of water molecules H-bonded to POPC phosphate and carbonyl oxygen atoms (H-bonded water), of water molecules in a clathrate around the choline group (choline water), of bound water molecules (H-bonded and choline water), of water bridges, and of charge pairs, per POPC in pure POPC, POPC-LA, and POPC-LAH bilayers and in leaflets containing more (m) and fewer (f) KP-23 molecules of POPC-LA and POPC-LAH bilayers (f, m). Errors in the average values are standard error estimates. For the pure POPC bilayer, differences between leaflets are within estimated errors, so only single average values are given.

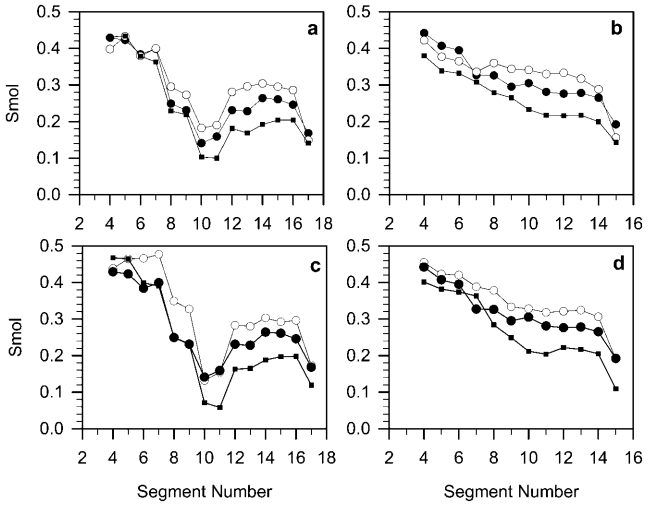

FIGURE 6 The molecular order parameter (S_{mol}) profiles calculated for β (*a* and *c*) and γ (*b* and *d*) chains of POPCs in both bilayer leaflets (*a*) and (*b*), respectively, and in the leaflet containing more KP-23 molecules (see text) (*c*) and (*d*), respectively, in pure POPC (●), POPC-LA (○), and POPC-LAH (■) bilayers at 310 K. The standard errors are less than the size of the symbols. Average values of S_{mol} are given in Table 2.

POPC-LA bilayer are mostly larger, whereas, in the POPC-LAH bilayer, are mostly smaller than those in the POPC bilayer. Both in POPC-LA and POPC-LAH bilayers, values of S_{mol} along the chain are higher for the leaflet containing more KP-23 molecules than for that containing fewer (Table 2). Thus, compared with the pure POPC bilayer, the PC chains in the POPC-LA bilayer are more ordered and in the POPC-LAH bilayer, less ordered. Even though properties of the interfacial region in POPC-LA and POPC-LAH bilayers are similar, the ordering of hydrocarbon chains is not.

Tilt of PC alkyl chains

An average tilt angle of a PC chain was calculated from cos^2 of the angle between the bilayer normal and the average segmental vector (Róg and Pasenkiewicz-Gierula, 2001a). Distributions of tilt angles of the β- and γ-chain in POPC-LA, POPC-LAH, and POPC bilayers are shown in Fig. 7. Shapes of distributions for both β- and γ-chain do not differ much among the bilayers; however, the fraction of β-chains with a small tilt is larger in the POPC-LA and smaller in the POPC-LAH bilayers than in the pure POPC bilayer. The fraction of β- and γ-chains with a large tilt is the largest in the POPC-LAH bilayer. As profiles of the *gauche* probability along the PC chain are similar in the three bilayers (data not shown), the small differences in PC chain tilts are responsible for the differences in S_{mol} profiles. In general, higher ordering of chains indicates their more tight packing. Thus, the PC chains in the POPC-LAH bilayer are less and in the POPC-LA bilayer are more tightly packed than in the pure POPC bilayer.

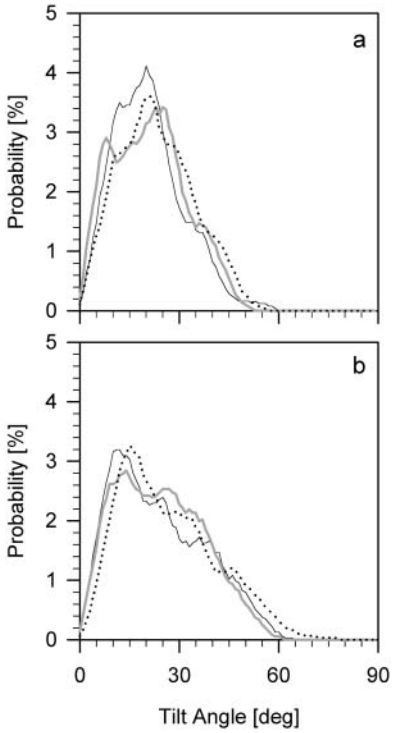

FIGURE 7 Distributions of tilt angles for β-chain (*a*), and γ-chain (*b*) in pure POPC (*thin*), POPC-LA (*thick*), and POPC-LAH (*dotted*) bilayers. Average tilt angles are given in Table 2.

DISCUSSION

Molecular dynamics simulations of phosphatidylcholine bilayers containing KP-23 molecules were carried out for several nanoseconds starting from nonequilibrium initial states (compare to Fig. 3). From a methodological point of view, the time covered in the simulations is relatively long, but the time is very short from a perspective of the process of local anesthesia. Nevertheless, in this initial period of time, several molecular events take place that relate to further stages of the process.

Both charged and uncharged forms of local anesthetic exist at physiological pH. Most likely, both forms are the active species (Bowman and Rand, 1980). The present study was undertaken to elucidate the atomic level interactions of LA with a hydrated PC bilayer and to show differences, if any, between interactions of neutral and protonated forms. The study demonstrated dissimilarities in interactions of both forms with PC and water molecules. The cause of these dissimilarities can be attributed to different amphiphilicity of protonated and neutral forms.

This study was not able to show any difference in the effect of KP-23S and KP-23R epimers on the bilayer. In general, stereoisomers differ in their biological activities (Triggle, 1997), but mainly due to their interactions with proteins. The POPC molecule that constituted the building block of the bilayer used in this study possesses only one

chiral center (C2) that is well hidden (compare to Fig. 1). It might be that cholesterol, which is present in a large amount in the plasma membrane of animal cells and possesses several chiral centers, could favor interaction with one chiral form of KP-23. However, to elucidate this effect additional studies are required.

In the present study, of the eight KP-23 molecules initially placed on the bilayer surface both in POPC-LA and POPC-LAH systems, a few, at least partially, intercalated into the bilayer. They located near the bilayer/water interface. Basic interactions responsible for such locations were different in each system. Neutral KP-23 molecules crossed the interfacial region and inserted some fragments into the bilayer core; their further penetration into the nonpolar region was restrained by interactions between polar groups of LA and POPC. Protonated KP-23 molecules did not cross the bilayer/water interface. Most of them self-condensed on the bilayer surface. The one that remained in the monomeric state, inserted its lipophilic carane head into the interfacial region, although formation of H-bonds between polar groups on its side chain and water precluded translocation of the molecule deeper into the bilayer.

Results of our study of the effect of KP-23 on the lipid bilayer are in line with experimental observations considered in the Introduction. In particular, partial intercalation of KP-23 into the lipid bilayer and decreased intercalation upon KP-23 protonation agree with data for other local anesthetics of Hata et al. (2000), Matsuki et al. (1998, 2001), Cadenhead (2001), Frangopol and Mihăilescu (2001), and de Paula and Schreier (1996). The larger mean distance between lipid headgroups in POPC bilayers containing KP-23, compared with this distance in the pure POPC bilayer, corresponds well with observations of Frangopol and Mihăilescu (2001). In accordance with the Ueda (2001) statement that interactions of local anesthetics with the bilayer are nonspecific, it was found that only few H-bonds between KP-23 and POPC polar groups were formed.

There is some disagreement in the literature concerning the effect of local anesthetics on the bilayer hydrocarbon chain region. Several reports indicate that uncharged local anesthetics decrease molecular organization of the egg PC bilayer (de Paula and Schreier, 1995; Pinot et al., 2000), whereas some other indicate that they increase the organization of micelles (Teixeira et al., 2001) and order of erythrocyte membranes (Frangopol and Mihăilescu, 2001). In this study, neutral KP-23 increased chain order/packing, whereas protonated KP-23 decreased chain order/packing of the POPC bilayer. The observed effect of neutral KP-23, which partially enters the bilayer core, may be compared to that of cholesterol, whose effect on the bilayer is to increase both the average distance between PC headgroups (Pasenkiewicz-Gierula et al., 2000) and chain packing (Róg and Pasenkiewicz-Gierula, 2001b). The effect of protonated KP-23 is not straightforward to explain. As in each leaflet of the bilayer only one LAH molecule locates in the interfacial region, the promoted increase of the available space to PC headgroups and chains by its presence is not large enough to decrease the chain order by the observed amount (Fig. 6). The only possibility remains that a large aggregate attached to the bilayer surface affects the chains order, but showing this quantitatively is not possible at this stage.

Smaller ordering of chains in leaflets containing fewer KP-23 molecules both in POPC-LA and POPC-LAH bilayers is most likely due to the chosen simulation conditions that keep the surface area of both bilayer leaflets the same (compare to Methods section).

The surface area available to a POPC headgroup is, on average, 2 $Å^2$/PC larger in POPC-LA and POPC-LAH bilayers than in the pure POPC bilayer. Nevertheless, higher PC-PC spacing in leaflets containing more KP-23 is accompanied by lower hydration of POPC headgroups. Decreased PC hydration in bilayers containing local anesthetics was observed experimentally, e.g., by Fourier transform infrared (FTIR) spectroscopy (Ueda et al., 1994). From FTIR spectra it was concluded that the NH groups of LAs replace some water molecules that were H-bonded to PC phosphate (Op) or carbonyl (Oc) oxygen atoms. Our study demonstrated that polar groups of neutral KP-23 molecules interact via H-bonding and electrostatic attraction with Op and Oc (compare to Fig. 5 *a*) and the average number of Op and Oc H-bonded water molecules in POPC-LA was by ~4% smaller than in the POPC bilayer (Table 3). This indicates that three LA molecules release seven H-bonded water molecules by replacing them or by screening Ops and Ocs from water. Protonated KP-23 changed the number of water molecules H-bonded to POPC also, although practically only one LAH molecule made H-bonds with POPC. This molecule was simultaneously H-bonded with Ops of three POPC molecules. Moreover, our study shows that both neutral and protonated KP-23 molecules decrease significantly the number of water molecules that clathrate the choline moiety. Clathrating water molecules are less strongly bound to PC than H-bonded ones and can more easily be displaced due to interactions with other groups. In conclusion, a decrease in hydration of the bilayer surface by KP-23 results from direct H-bonding between KP-23 and PC (compare to Fig. 5 *a*) and screening of PC polar groups by KP-23. The effect of the protonated form is slightly stronger than that of the neutral form (compare to Table 3). Compared to a pure POPC bilayer, the increased surface area is not accompanied by higher hydration of PC headgroups in leaflets containing only one KP-23 molecule. This is because PC hydration is limited by the capacity of the PC polar groups to interact with water and shows saturation for the surface area of ~64 $Å^2$/PC (Róg and Pasenkiewicz-Gierula, 2003).

It has been shown experimentally (Matsuki et al., 1998, and references cited therein) that positively charged local anesthetics undergo self-association in aqueous solutions and form micelle-like molecular aggregates. In the presence

of a membrane, self-association may take place at the membrane surface. Ueda et al. (1994) indicated that anesthetic potency is related to cooperative condensation of anesthetic molecules at the membrane interface. In our MD simulation study, neutral KP-23 molecules formed a smaller aggregate in a head-to-tail-like arrangement that was immersed in water, whereas protonated KP-23 molecules formed a much larger, micelle-like aggregate that was anchored to the bilayer surface via H-bonds between one LAH and three POPC molecules. This particular LAH molecule remained on the bilayer surface from the onset of the simulation and the other six molecules slowly condensed on it (compare to Fig. 4 *b*). The aggregation of KP-23 molecules in POPC-LA and POPC-LAH systems might be an additional cause of a lower hydration of POPC headgroups in these bilayers as compared to the hydration in pure POPC bilayers. Side chains of both neutral and protonated KP-23 contain polar and hydrophobic groups. These groups, when exposed on surfaces of the aggregates, enforce reorientation and hinder mobility of the nearby water; in effect, water readiness to interact with the bilayer lipids decreases. Particularly affected might be water molecules that are weakly bound to PC, like those forming clathrates around the choline group.

In conclusion, KP-23 molecules in neutral and protonated forms decreased hydration of PC headgroups by 6 and 10%, respectively, whereas their effect on the PC hydrocarbon chain order was the opposite. In the water phase, both forms aggregated by self-association, but the size and character of the aggregates were different. The aggregate of the protonated species was adsorbed on the bilayer surface, whereas that of the neutral ones was immersed in water. Partial dehydration of the bilayer surface by local anesthetic molecules and their cooperative condensation on the bilayer surface, observed in this computer simulation study, were among the postulated mechanisms of local anesthetics action (Ueda et al., 1994, and references cited therein). In this sense, the results reported here conform to experimental findings, despite the limited size of the computer models. But the main advantage of MD simulations is that they describe in atomic level detail the effect of a representative local anesthetic on the phospholipid bilayer. This detail, often not available from observation, may be helpful in the interpretation of a large body of experimental data. Another interesting result of our study is the demonstration that the processes involving local anesthetics take actually place on a rapid timescale near the bilayer/water interface.

T.R. holds a fellowship award from the Polish Foundation for Science. This study was supported in part by grant S4P05F01916 and 6P04A03121from the Committee for Scientific Research, Poland. Some calculations were performed at the Academic Computer Center Cyfronet, Poland, under grant KBN/sgi_origin_200/UJ/004/2000. Crystallographic measurements using synchrotron radiation were done under Hamburger Synchrotronstrahlungslabor am Deutschen Elektronen-Synchrontron (DESY-HASYLAB) project I-00-024.

REFERENCES

Berendsen, H. J. C., J. P. M. Postma, W. F. van Gunsteren, A. DiNola, and J. R. Haak. 1984. Molecular dynamics with coupling to an external bath. *J. Chem. Phys.* 81:3684–3690.

Bowman, W. C., and M. J. Rand. 1980. Textbook of Pharmacology. Blackwell Scientific Publication, Oxford, UK.

Cadenhead, D. A. 2001. Model membrane/substrate interactions: ethanol and procaine interactions. *Coll. Surf. B.* 22:63–68.

Case, D. A., D. A. Pearlman, J. W. Caldwell, T. E. Cheatham III, W. S. Ross, C. Simmerling, T. A. Darden, K. M. Merz, R. V. Stanton, A. L. Cheng, J. J. Vincent, M. Crowley, D. M. Ferguson, R. J. Radmer, G. L. Seibel, U. C. Singh, P. K. Weiner, and P. A. Kollman. 1997. AMBER 5.0. University of California, San Francisco.

Czarnecki, R., K. Czerwińska, K. Grochowska, J. Grochowski, T. Librowski, and P. Serda. 1992. Molecular structure and antiaggregating activity of a potent local anaesthetic (–)-4-[2-hydroxy-3-(*n*-isopropylamino)-propoxyimino]-*cis*-carane. *Arzneimittel-Forsh.* 42:1279–1283.

de Paula, E., and S. Schreier. 1995. Use of a novel method for determination of partition coefficients to compare the effect of local anesthetics on membrane structure. *Biochim. Biophys. Acta.* 1240:25–33.

de Paula, E., and S. Schreier. 1996. Molecular and physicochemical aspects of local anesthetic-membrane interaction. *Braz. J. Med. Biol. Res.* 29:877–894.

1995. DISCOVER User Guide. Biosym/MSI, San Diego, CA.

Egberts, E., S.-J. Marrink, and H. J. C. Berendsen. 1994. Molecular dynamics simulation of a phospholipid membrane. *Eur. Biophys. J.* 22: 423–436.

Essmann, U., L. Perera, M. L. Berkowitz, T. Darden, H. Lee, and L. G. Pedersen. 1995. A smooth particle mesh Ewald method. *J. Chem. Phys.* 103:8577–8593.

Frangopol, P. T., and D. Mihăilescu. 2001. Interactions of some local anesthetics and alcohols with membranes. *Coll. Surf. B.* 22:3–22.

Grochowski, J., P. Serda, M. Pasenkiewicz-Gierula, R. Czarnecki, T. Librowski, S. Lochyński, B. Frąckowiak, C. Baehtz, and M. Knapp. 2001. Enantiopurity/Epimeric Disorder Studies of a New Local Anesthetic using SR HRPD. *HASYLAB Jahresbericht.* 471–472.

Grochowski, J., P. Serda, M. Pasenkiewicz-Gierula, R. Czarnecki, T. Librowski, S. Lochyński, and B. Frąckowiak. 2002. Structural characterization of carane derivative stereoisomers—potent local anesthetics. *Acta. Phys. Pol. A.* 101:665–674.

Gupta, S. P. 1991. Quantitative structure-activity relationship studies of local anesthetics. *Chem. Rev.* 91:1109–1119.

Hata, T., T. Sakamoto, H. Matsuki, and S. Kaneshina. 2000. Partition coefficients of charged and uncharged local anesthetics into dipalmitoylphosphatidylcholine bilayer membrane: estimation of PH dependence on the depression of phase transition temperatures. *Coll. Surf. B.* 22: 77–84.

Heller, H., M. Schaefer, and K. Schulten. 1993. Molecular dynamics simulation of a bilayer of 200 lipids in the gel and liquid-crystal phases. *J. Phys. Chem.* 97:8343–8360.

Hubbell, W. L., and H. M. McConnell. 1971. Molecular motion in spin-labeled phospholipids and membranes. *J. Am. Chem. Soc.* 93:314–326.

Jorgensen, W. L., and J. Tirado-Rives. 1988. The OPLS potential functions for proteins. Energy minimizations for crystals of cyclic peptides and crambin. *J. Am. Chem. Soc.* 110:1657–1666.

Jorgensen, W. L., J. Chandrasekhar, J. D. Madura, R. W. Impey, and M. L. Klein. 1983. Comparison of simple potential functions for simulating liquid water. *J. Chem. Phys.* 79:926–935.

Librowski, T., R. Czarnecki, M. Pasenkiewicz-Gierula, J. Grochowski, P. Serda, S. Lochyński, and B. Frąckowiak. 2000. Multidisciplinary studies of chiral carane derivatives with a strong local anaesthetic activity. *Euro. J. Pharm. Sci.* 11:113–114.

Lochyński, S., B. Frąckowiak, T. Librowski, R. Czarnecki, J. Grochowski, P. Serda, and M. Pasenkiewicz-Gierula. 2002. Stereochemistry of terpene derivatives. III. Hydrolytic kinetic resolution as a convenient approach to

chiral aminohydroxyiminocaranes with local anesthetic activity. *Tetrahedr. Asym.* 13:873–878.

Matsuki, H., T. Hata, M. Yamanaka, and S. Kaneshina. 2001. Partitioning of uncharged local anesthetic benzocaine into model biomembranes. *Coll. Surf. B.* 22:69–76.

Matsuki, H., M. Yamanaka, S. Kaneshina, H. Kamaya, and I. Ueda. 1998. Surface tension study on the molecular-aggregate formation of local anesthetic dibucaine hydrochloride. *Coll. Surf. B.* 11:87–94.

Murzyn, K., T. Róg, G. Jezierski, Y. Takaoka, and M. Pasenkiewicz-Gierula. 2001. Effects of phospholipid unsaturation on the membrane/water interface: a molecular simulation study. *Biophys. J.* 81:170–183.

Ohki, S., and H. Ohshima. 1996. Distribution of local anesthetics in lipid membrane. *Coll. Surf. B.* 5:291–305.

Ohta-Ino, S., M. Pasenkiewicz-Gierula, Y. Takaoka, H. Miyagawa, K. Kitamura, and A. Kusumi. 2001. Fast lipid disorientation at the onset of membrane fusion revealed by molecular dynamics simulation. *Biophys. J.* 81:217–224.

Pasenkiewicz-Gierula, M., Y. Takaoka, H. Miyagawa, K. Kitamura, and A. Kusumi. 1997. Hydrogen bonding of water to phosphatidylcholine in the membrane as studied by a molecular dynamics simulation: location, geometry and lipid-lipid bridging via hydrogen bonded water. *J. Chem. Phys.* 101:3677–3691.

Pasenkiewicz-Gierula, M., Y. Takaoka, H. Miyagawa, K. Kitamura, and A. Kusumi. 1999. Charge pairing of headgroups in phosphatidylcholine membranes: a molecular dynamics simulation study. *Biophys. J.* 76: 1228–1240.

Pasenkiewicz-Gierula, M., T. Róg, K. Kitamura, and A. Kusumi. 2000. Cholesterol effects on the phosphatidylcholine bilayer polar region: a molecular simulation study. *Biophys. J.* 78:1376–1389.

Pinot, L. M. A., D. K. Yokaichiya, L. F. Fraceto, and E. de-Paula. 2000. Interaction of benzocaine with model membrane. *Biophys. Chem.* 87: 213–223.

Róg, T., and M. Pasenkiewicz-Gierula. 2001a. Cholesterol effects on the phosphatidylcholine bilayer nonpolar region: a molecular simulation study. *Biophys. J.* 81:2190–2202.

Róg, T., and M. Pasenkiewicz-Gierula. 2001b. Cholesterol effects on the membrane packing and condensation: a molecular simulation study. *FEBS Lett.* 502:68–71.

Róg, T., and M. Pasenkiewicz-Gierula. 2003. Effects of epicholesterol on the phosphatidylcholine bilayer: a molecular simulation study. *Biophys. J.* 84:1818–1226.

Ryckaert, J. P., G. Ciccotti, and H. J. C. Berendsen. 1977. Numerical integration of the Cartesian equations of motion of a system with constraints: molecular dynamics of *n*-alkanes. *J. Comp. Phys.* 23:327–341.

Seelig, J., and N. Waespe-Šarčević. 1978. Molecular order in *cis* and *trans* unsaturated phospholipid bilayers. *Biochemistry.* 17:3310–3315.

Seelig, J., and A. Seelig. 1980. Lipid conformation in model membranes and biological membranes. *Q. Rev. Biophys.* 13:19–61.

Siemieniuk, A., H. Szałkowska-Pągowska, S. Lochyński, K. Piątkowski, B. Filipek, R. Czarnecki, T. Librowski, and S. Białas. 1992. Synthesis and some pharmacological properties of 1,2-amino ethers with natural monoterpene structures. *Pol. J. Pharmacol.* 44:187–200.

Teixeira, C. V., R. Itri, F. Casallanovo, and S. Schreier. 2001. Local anesthetic-induced microscopic and mesoscopic effects in micelles: a fluorescence, spin label and SAXS study. *Biochim. Biophys. Acta.* 1510:93–105.

Triggle, D. J. 1997. Stereoselectivity of drug action. *Drug Discov. Today.* 2:138–147.

Ueda, I. 2001. Molecular mechanisms of anesthesia. *Keio J. Med.* 50: 20–25.

Ueda, I., J.-S. Chiou, P. R. Krishna, and H. Kamaya. 1994. Local anesthetics destabilize lipid membranes by breaking hydration shell: infrared and calorimetry studies. *Biochim. Biophys. Acta.* 1190:421–429.